CNR-INO
ISTITUTO NAZIONALE DI OTTICA
CONSIGLIO NAZIONALE DELLE RICERCHE

Laser-Driven Electron and Ion Acceleration: Established Results and Progress

M. Salvadori, F. Avella, F. Baffigi, G. Bandini, F. Brandi, G. Cristoforetti, M. Ezzat, A. Fregosi, L. Fulgentini, D. Gregocki, L. Labate, P. Koester, D. Palla, S. Piccinini, S. Vlachos and L. A. Gizzi

Conferenza Italiana sui Plasmi (CIP) 2026, Frascati

Intense Laser Irradiation Laboratory (ILIL)

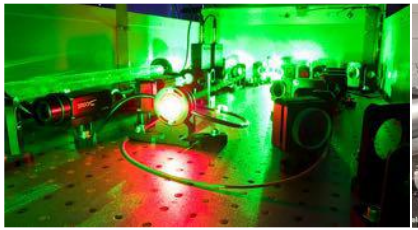

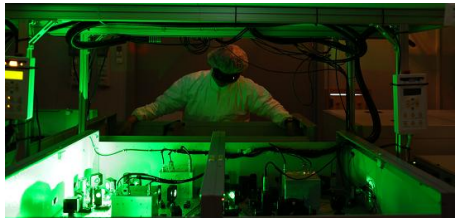

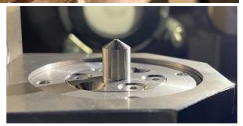

LASER DEV. LAB

USER CONTROL ROOM

TESTING AND PROTOTYPING

LASER FRONT END

POWER AMPLIFIER Up to 240 TW

SHIELDED TARGET AREA FOR PARTICLE ACCELERATION

NEW BEAMLINE FOR PRE-CLINICAL STUDIES

NEW HIGH DOSE UNDERGROUND BUNKER

LASER CAPABILITIES:

- 220 TW, Ti:Sa, up to 5 Hz, 23 fs;
- 1kHz ≤20 mJ Ti:Sa + ≤ 2 mJ OPA @ 2μm
- 100 Hz, ~1J, TiSA (procurement in progress)

L. A. Gizzi et al., High Power Laser Science and Engineering, 9 e10 (2021)

ILIL: Group Members and Activities

Main Activities carried out in our group

→ Laser-Plasma Interaction in condition relevant for ICF
→ Laser-driven electron acceleration and applications
→ Laser-driven Ion acceleration and applications
→ Laser developments

Leonida A. **GIZZI*** (Head of lab)
Fernando **BRANDI**
Gabriele **CRISTOFORETTI**
Petra **KOESTER**
Luca **LABATE***
Federica **BAFFIGI**
Lorenzo **FULGENTINI**
Gabriele **BANDINI** (term)
Mohamed **EZZAT** (term)

Alessandro **FREGOSI** (term)
Daniele **PALLA** (term)
Simona **PICCININI** (term)
Martina **SALVADORI** (term)
Federico **AVELLA** (PhD student)
David **GREGOCKI** (PhD student)
Simon **VLACHOS** (PhD student)
Caterina **MOZZO** (PhD student)
Gianluca **CELLAMARE** (associated)

**also at INFN*

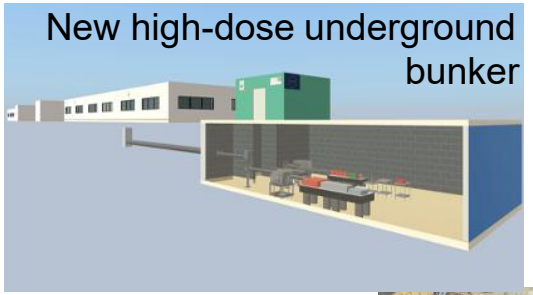

construction undergoing as we speak…

ILIL: Group Members and Activities

Main Activities carried out in our group

→ **Laser-Plasma Interaction in condition relevant for ICF**
→ Laser-driven electron acceleration and applications
→ Laser-driven Ion a
→ Laser developmer

Follow **P. Koester** Talk on **Thursday 5th at 10 am**
«Fusion energy research with high power lasers in Europe: the HiPER+ programme»

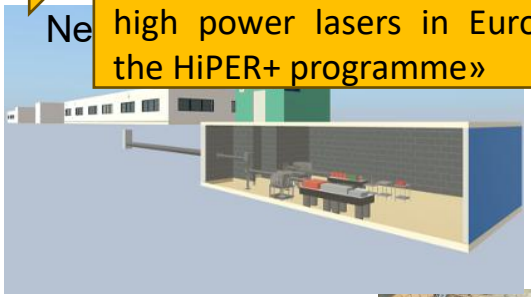

construction undergoing as we speak…

Leonida A. **GIZZI*** (Head of lab)
Fernando **BRANDI**
Gabriele **CRISTOFORETTI**
Petra **KOESTER**
Luca **LABATE***
Federica **BAFFIGI**
Lorenzo **FULGENTINI**
Gabriele **BANDINI** (term)
Mohamed **EZZAT** (term)

Alessandro **FREGOSI** (term)
Daniele **PALLA** (term)
Simona **PICCININI** (term)
Martina **SALVADORI** (term)
Federico **AVELLA** (PhD student)
David **GREGOCKI** (PhD student)
Simon **VLACHOS** (PhD student)
Caterina **MOZZO** (PhD student)
Gianluca **CELLAMARE** (associated)

****also at INFN***

In this Talk:

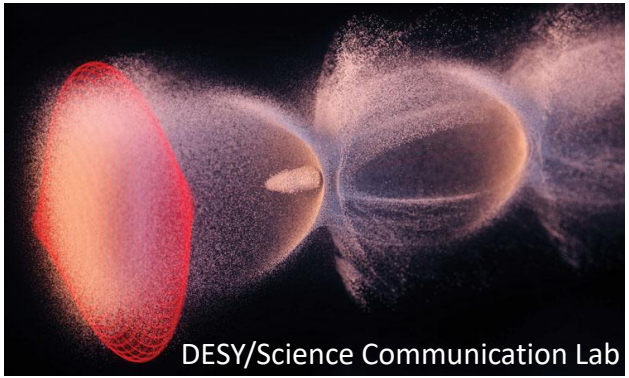

Laser Driven Electron Acceleration

Brief Introduction and Basic concepts

Application to UHDR radiotherapy

Laser Driven Ion Acceleration

Brief Introduction and Basic concepts

Applications Material Analysis & Radioisotope production

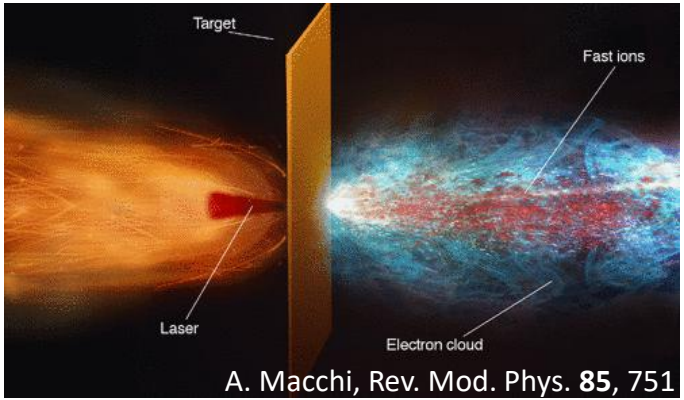

Laser-Driven electron Acceleration: wake field generation

Why plasma-based accelerator ?

- Possibility to reach extremely high acceleration gradients → Compactness
- Short temporal duration of the accelerated e^- bunch

The **acceleration mechanism relies on the excitation of plasma waves**: In laser-driven acceleration the driver of the perturbation is the laser.

The electric field of the laser exerts a force on ions and electrons

Electrons, being lighter, cover a larger distance →Charge separation is induced

Electrons starts to oscillate around the equilibrium position with the characteristic ω_p

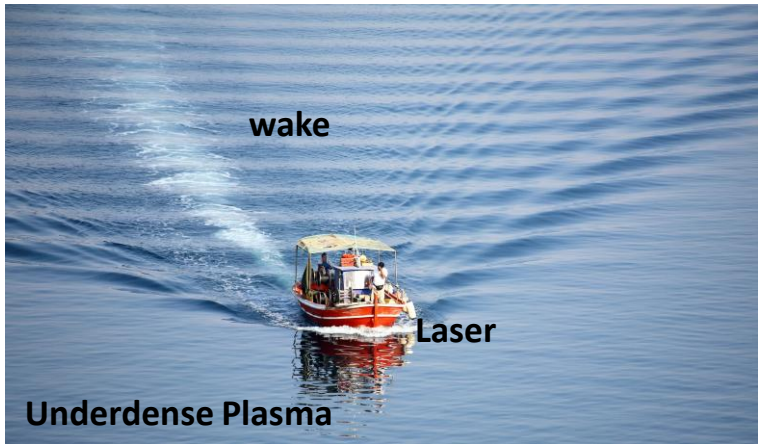

Laser-Driven electron Acceleration: wakefield generation

According to the laser intensity it is possible to distinguish among two different regimes:

- Linear regime $a_o = \frac{eE_L}{m_e \omega_L c} \ll 1$

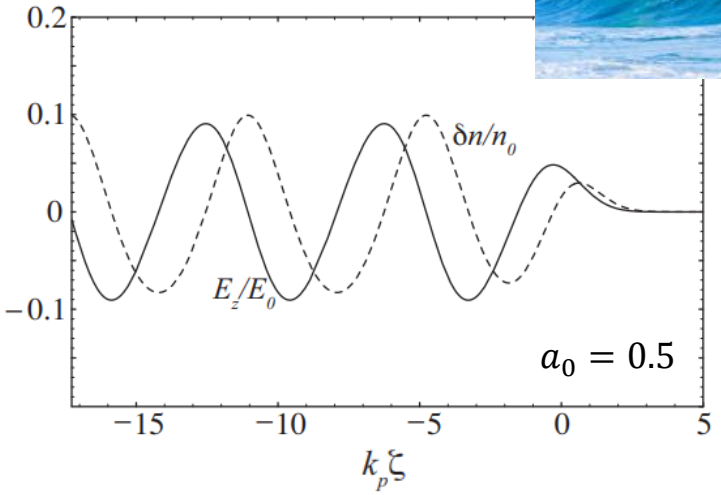

- Non- Linear regime $a_o \geq 1$

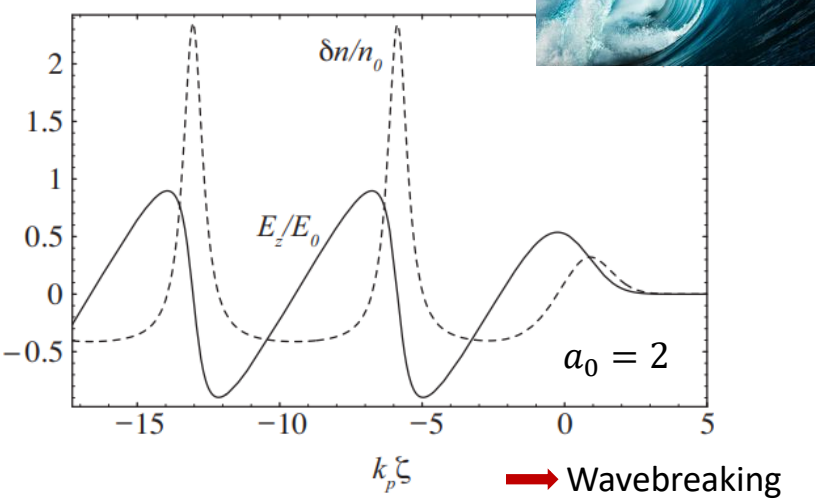

➡ Wavebreaking

E. Esarey et al., RevModPhys 81 (2009)

Laser wakefield acceleration: Blow-out Regime and Self Injection

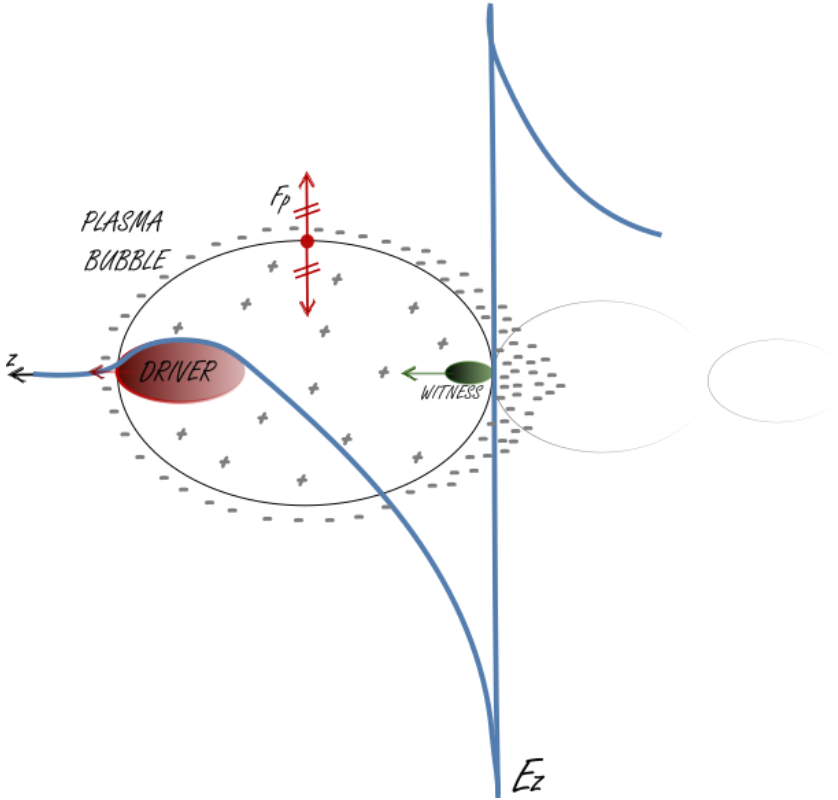

High intensity laser exerts ponderomotive forces on plasma charges, the high intensity allows for complete depletion of electrons from the axis.

The empting zone is referred to as the «bubble»

As the laser pulse propagates in the plasma, electrons are accumulated at the rear side of the bubble

In this region the accelerating electric field can be strong enough to trap background plasma electrons in the bubble → **Self Injection**

Laser wakefield acceleration: Blow-out Regime

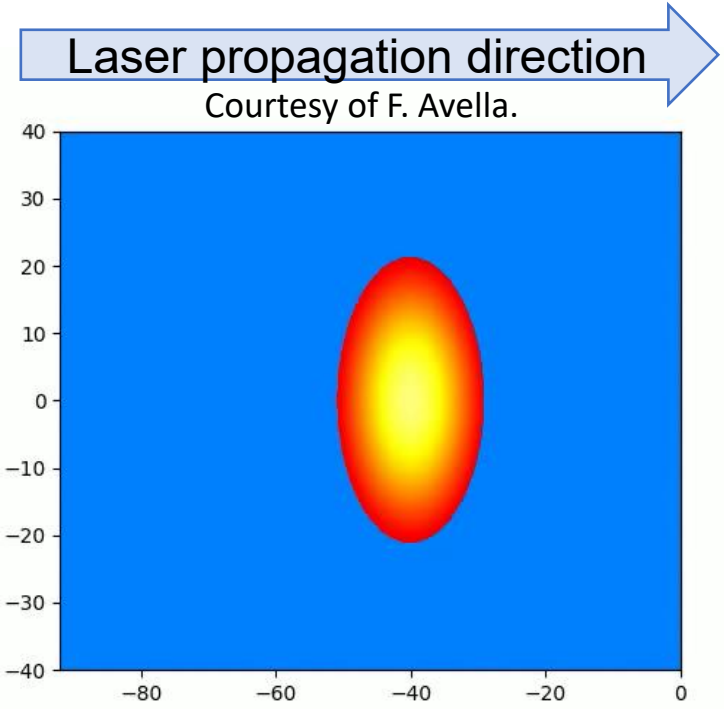

Laser wakefield acceleration: Blow-out Regime

Laser propagation direction

Courtesy of F. Avella.

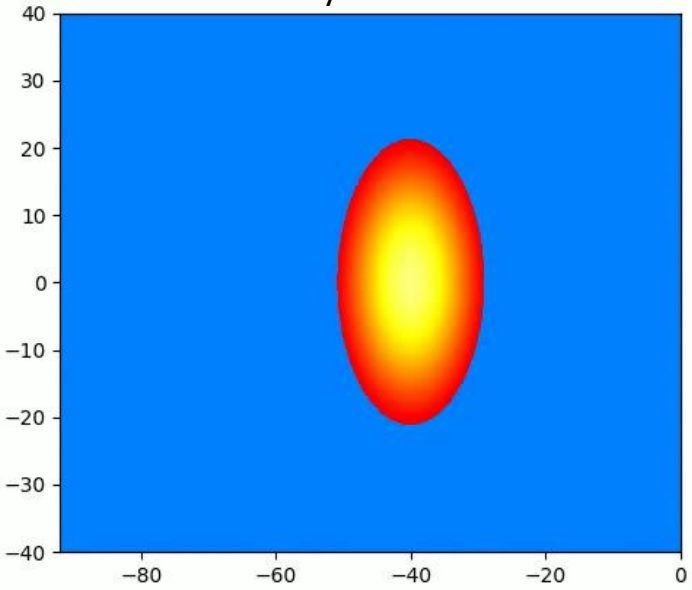

self injection relies on trapping background plasma electrons → electrons on the tail of thermal distribution may have a sufficient momentum to be on a trapped orbit

→ High energy spread and emittance

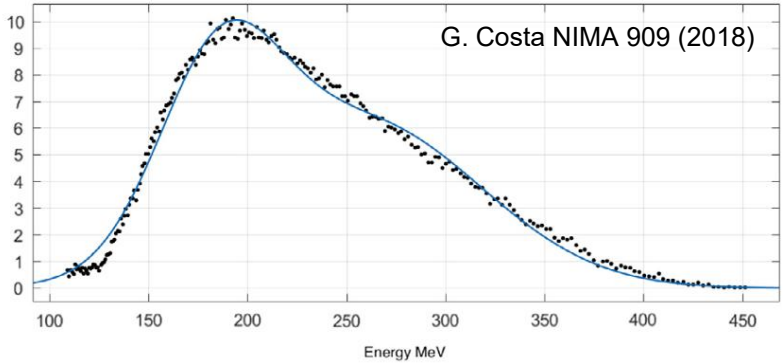

Different methods have been proposed to control the injection process so to achieve higher quality electron bunches (i.e. laser triggered injection, density tailoring…)

Laser wakefield acceleration: Ionization Injection

Ionization triggered injection is achieved by ionizing deeply bounded electrons of an high atomic number gas at a proper phase inside the laser driven wakefield

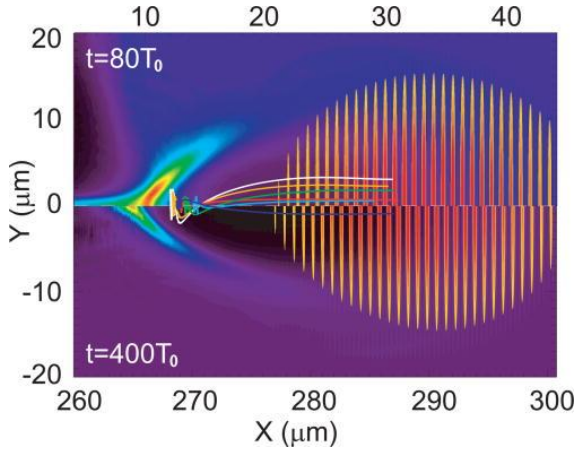

→ The idea is to irradiate a gas mixture made primarly of a low Z gas (i.e. 99% H) with a small amount of a high Z gas (i.e. 1% N).

The **ionization of the low Z gas**, achieved by the leading edge of the laser, will generate the **plasma wave oscillations**. On the other hand, the inner shell **electrons of the high-Z gas** require an higher electric field to be ionized → near the peak of the laser intensity. Therefore they are **ionized, pomptly trapped and accelerated.**

→ high quality beams with lower energy spread and emittance of accelerated electrons is achieved

Chen, PoP 19,033101 (2012)

Laser Wakefield Acceleration at ILIL

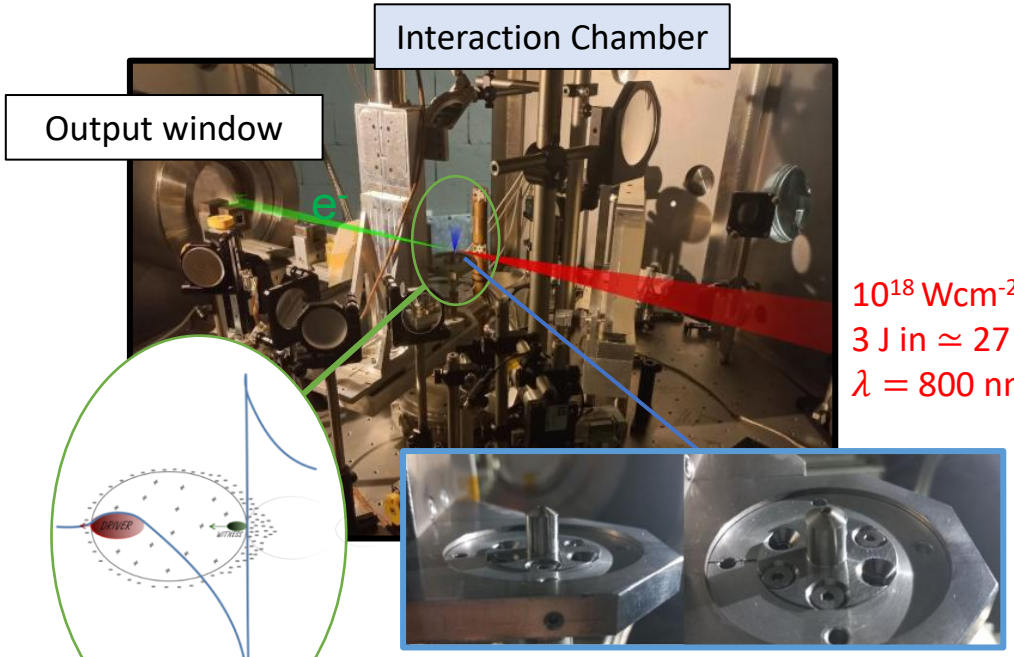

10^{18} Wcm^{-2}
3 J in ≃ 27 fs
$\lambda = 800$ nm

Supersonic flow of Helium Gas with 1% Nitrogen
LWFA ⟹ Ionization Injection
Operative electron density ≃ $10^{18}\ cm^{-3}$

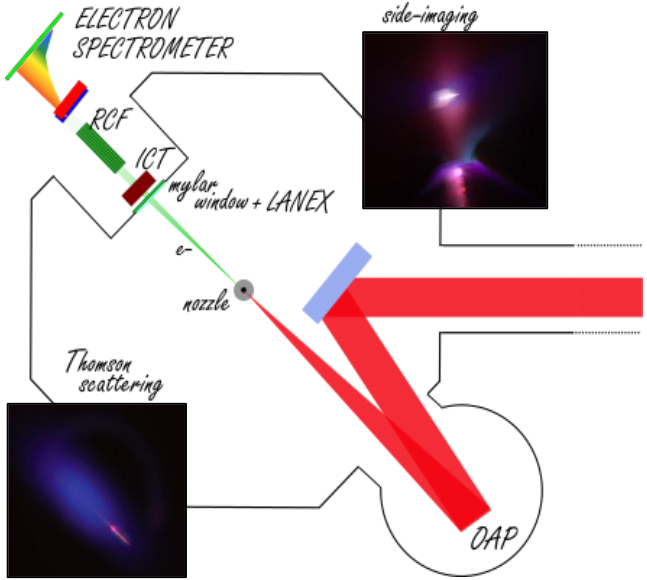

Beam Charge | Beam Spectra

Beam Size and Pointing

Dose and DPP

Laser Wakefield Acceleration at ILIL

Beam Spectra

S.G. Vlachos NIMA 1082:2 (2026)

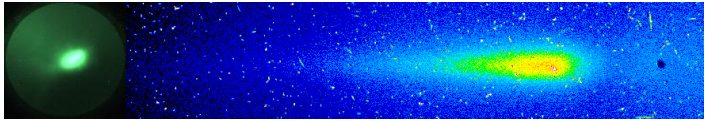

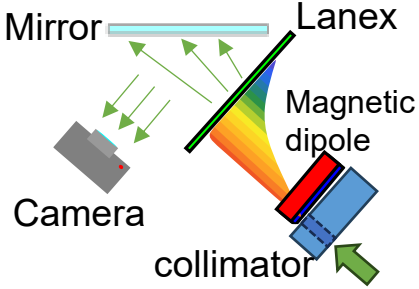

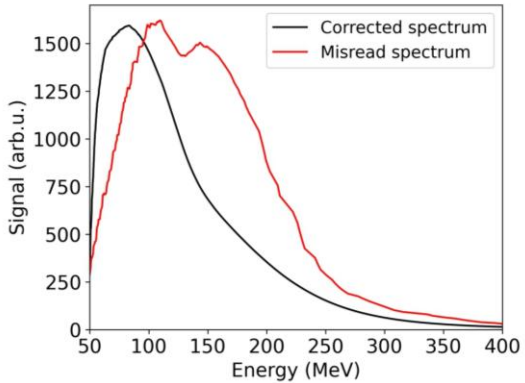

Dose and DPP

Courtesy of S. Piccinini

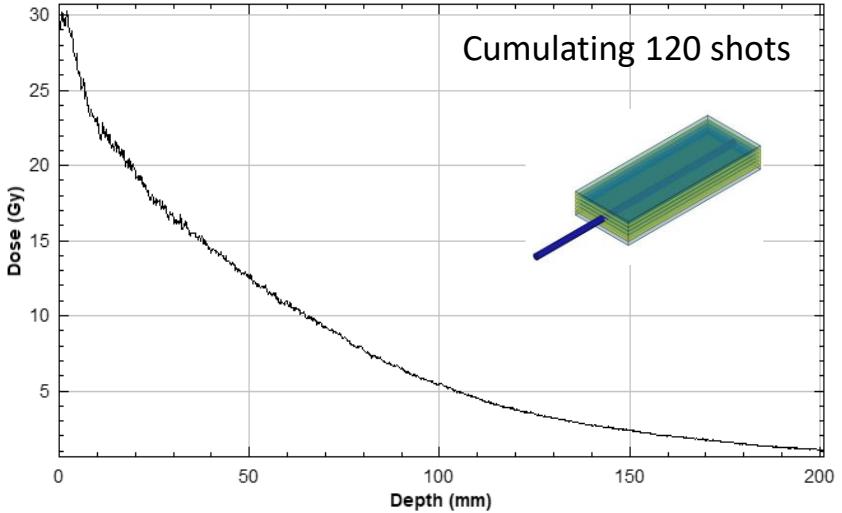

Beam Size and Pointing stability

$r_x \sim 1.15$ cm, $r_y \sim 0.9$ cm at ~ 60 cm from the source

$\sigma_x \sim 2$ mm, $\sigma_y \sim 2.8$ mm

Beam Charge $\simeq 150\ pC$

D. Gregocki Instruments **2025**, 9(4), 25

Laser Wakefield Acceleration at ILIL

Beam Spectra S.G. Vlachos NIMA 1082:2 (2026)

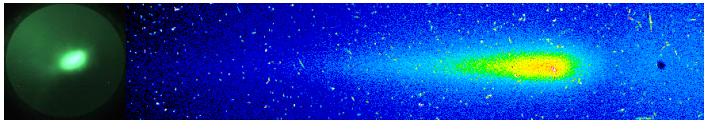

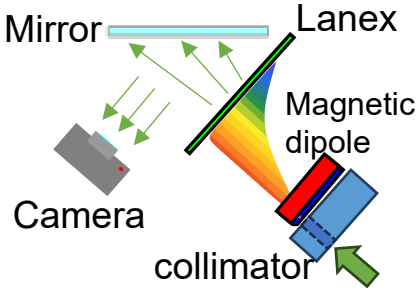

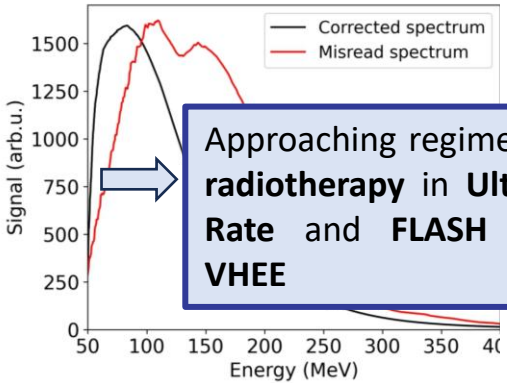

Approaching regimes relevant for **radiotherapy** in **Ultra High dose Rate** and **FLASH** regime with **VHEE**

Dose and DPP Courtesy of S. Piccinini

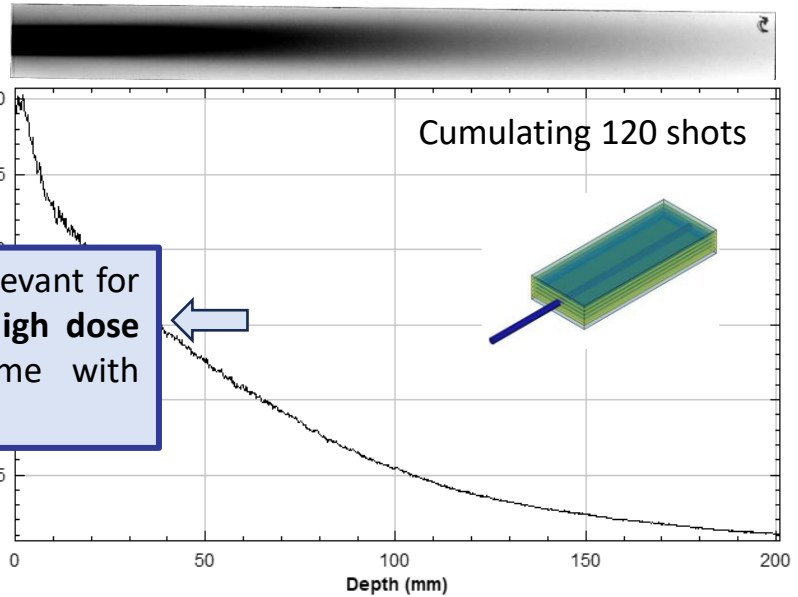

Beam Size and Pointing stability

$r_x \sim 1.15$ cm, $r_y \sim 0.9$ cm at ~ 60 cm from the source

$\sigma_x \sim 2$ mm, $\sigma_y \sim 2.8$ mm

Beam Charge $\simeq 150\ pC$

D. Gregocki Instruments **2025**, 9(4), 25

LWFA VHEE for UHDR radiotherapy

VHEE (50 MeV < E < 250 MeV):
+ Suitable for deep-seated tumors
+ Sharp beam penumbra
+ Low sensitivity to inhomogeneities
- High entrance and exit dose

Main objective: damage enhancement to the targeted volume (cancer cells) while sparing the nearby tissues and OAR (organ at risk)

→ Need for dosimetric characterization

Investigation of dose deposition in complex geometry such as Multi Field Irradiation (MFI) and Intensity Modulation (IM) schemes.

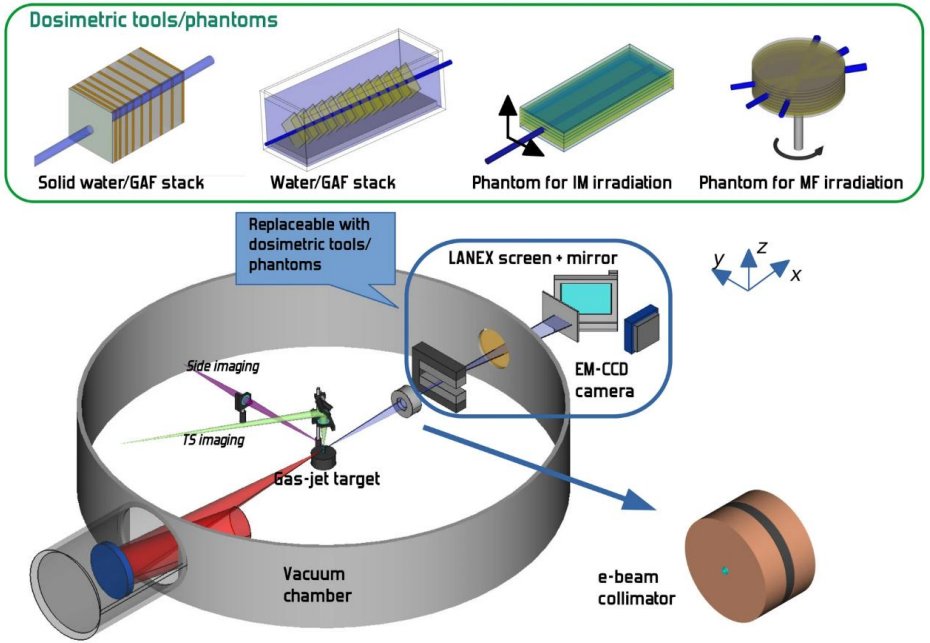

120 pc/shot
Spectral energy distribution within 50-250 MeV

L. Labate et al, Sci Rep 10, 17307 (2020). *C. M. V. Panaino Cancers* **2025**, *17*(2), 181

LWFA VHEE for UHDR radiotherapy

Multi Field Irradiation

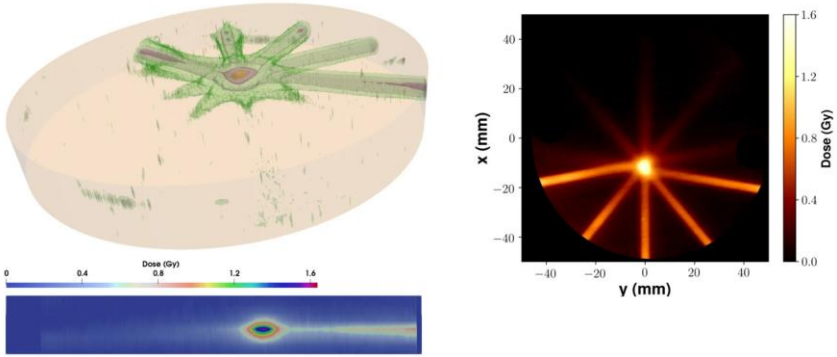

GAF chromic sandwiched in 2 mm Polycarbonate disks

Rotating Cylinder along the z-axis,
accumulating same number of shots every 40 rotation
Targeted volume received:
→ 2.5 times the entrance dose,
→ 3-4 times the dose in the surrounding volume,
→ 16 times the exit dose.

Intensity Modulation

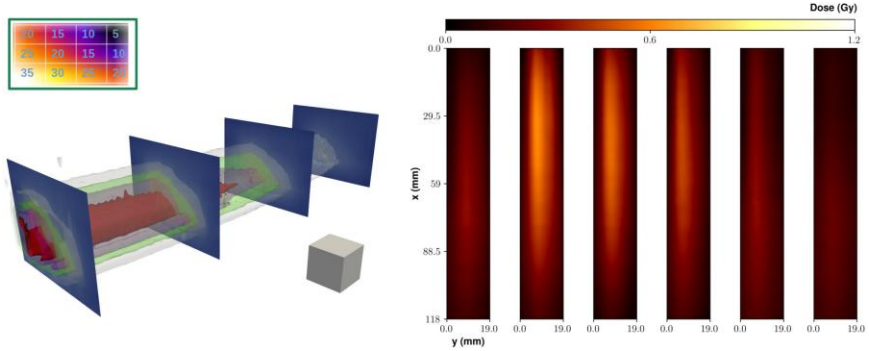

Irradiation Map → 3 mm x 4 mm matrix
Each slot received a different number of shots

Measured dose gradient both in the x and y direction

→ Possibility to have a localized dose deposition

L. Labate et al, Sci Rep **10**, 17307 (2020).

VHEE for FLASH radiotherapy

FLASH-RT: delivering **high doses** in an extremely **short irradiation time** (Dose rate > 40 Gy/s)

LWFA-VHEE → Extremely short bunch duration

VHEE FLASH-RT → dosimetric characteristic combined to the sparing capability of FLASH

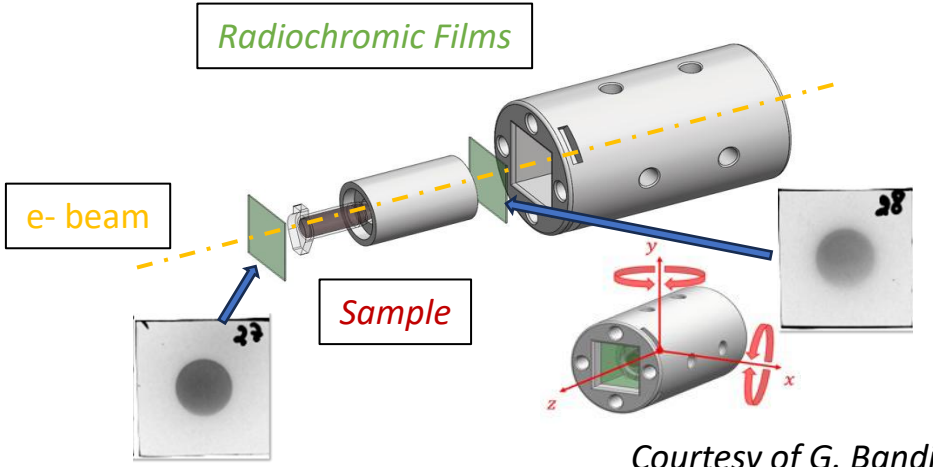

Courtesy of G. Bandini

Human peripherical blood irradiation

Evaluation of the dose-response curve of Peripheral blood lymphocytes DNA damage due to laser-guided ultra-high dose rate VHEE pulses irradiation

Radiobiological endpoints

- **Micronucleus Test**
- **Telomere Shortening**

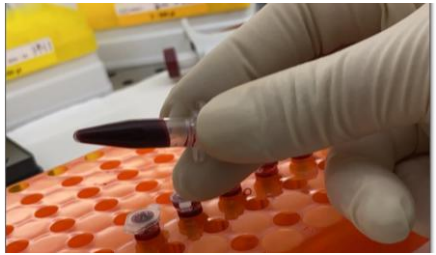

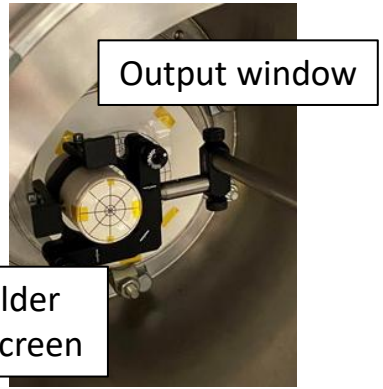

LWFA for FLASH radiotherapy

Micronucleus Test: gold standard for evaluating radiation-induced chromosomal damage.
The assessment cover both **targeted** and **bystander** effects.

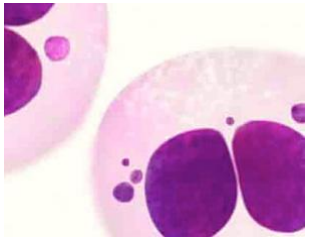

Telomere Shortening: Analysis of telomere length as an indicator of radiation-induced genomic instability.

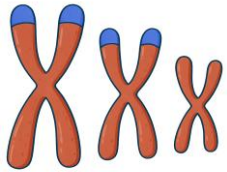

VHEE (10^{12} Gy/s per pulse)

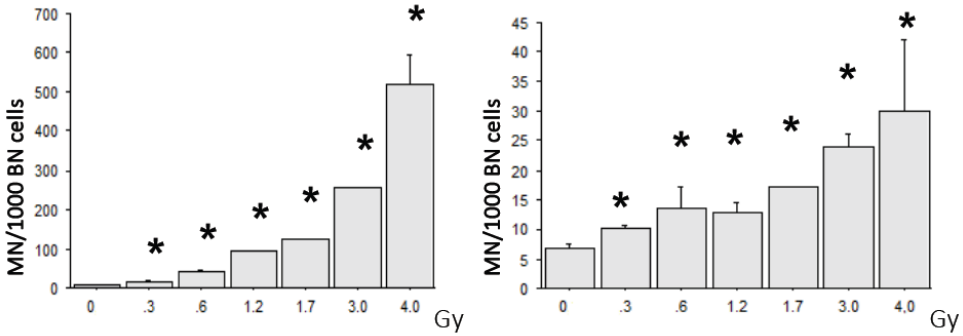

VHEE (10^{12} Gy/s per pulse) - TL

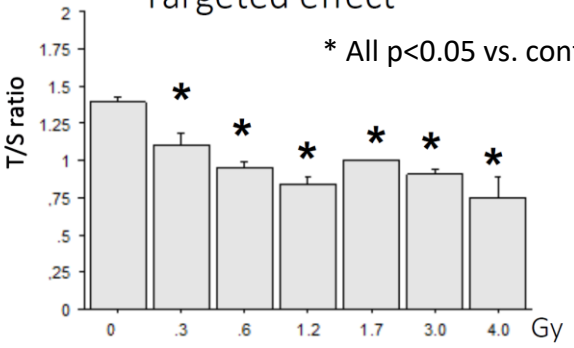

Courtesy of S. Piccinini, A. Borghini

Many mechanisms investigated, many results obtained…

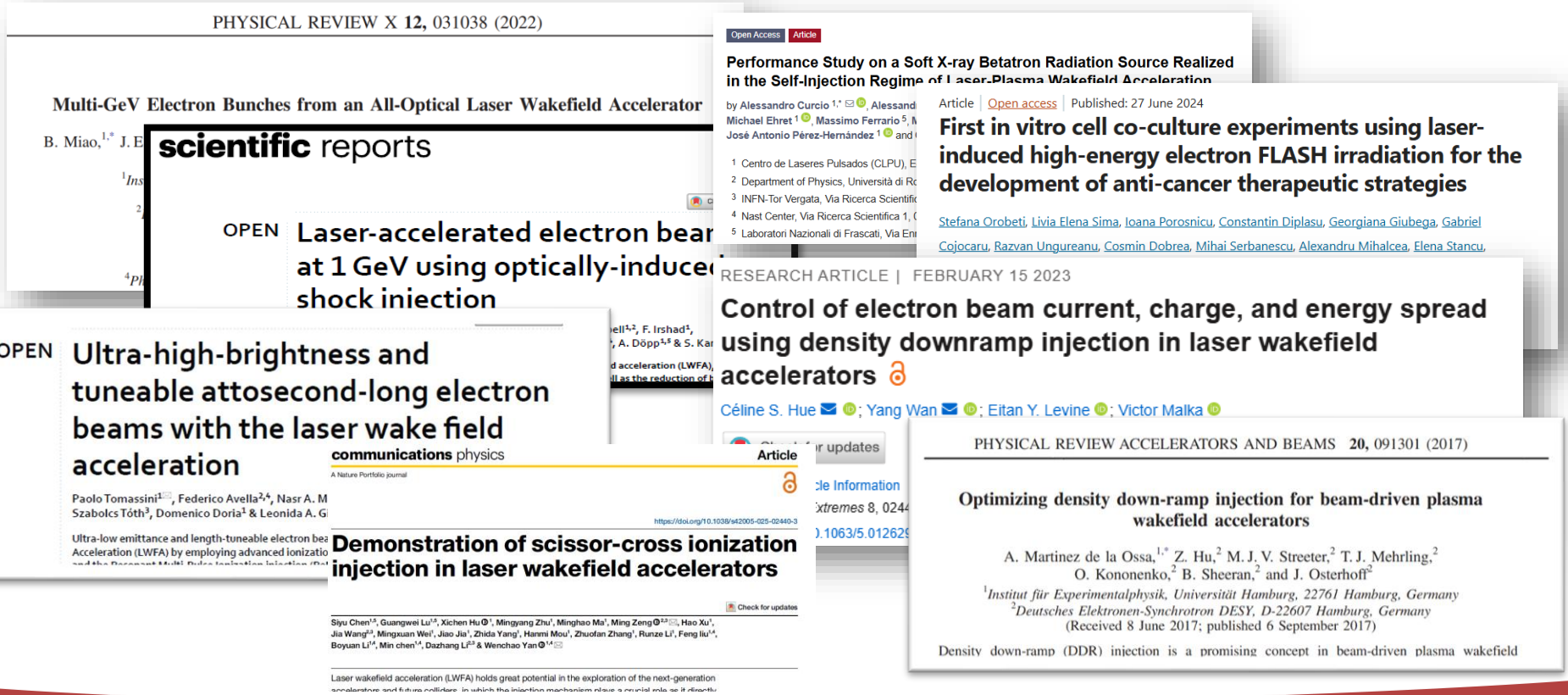

Laser Driven Ion Acceleration

Short, high power laser interacting with solid thin targets (flat foil, nanostructured, ultrathin foil…)

Depending on the specific laser parameters and target characteristics different acceleration mechansim can prevail

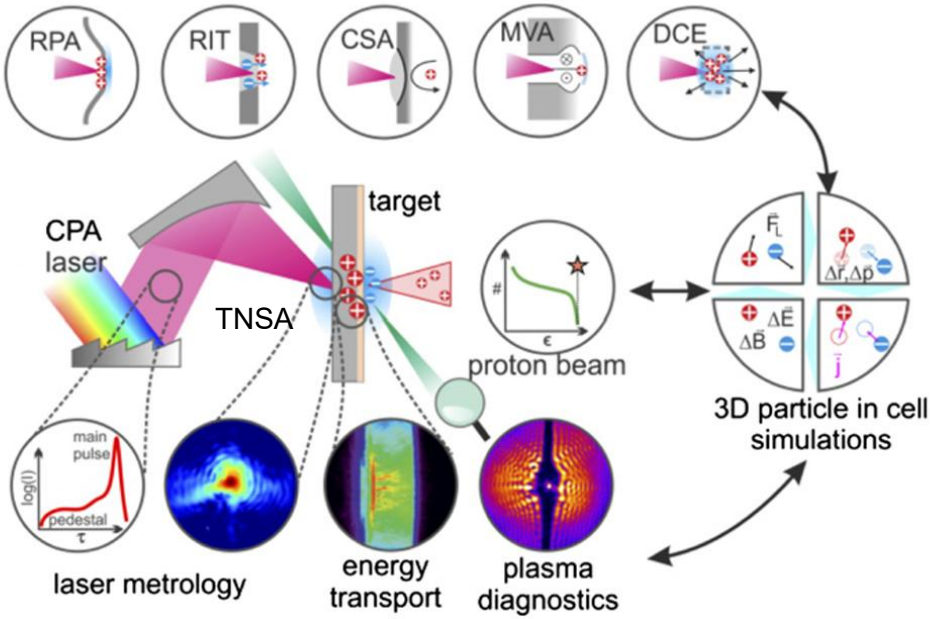

F. Albert et al 2021 New J. Phys. 23 031101

Laser Driven Ion Acceleration

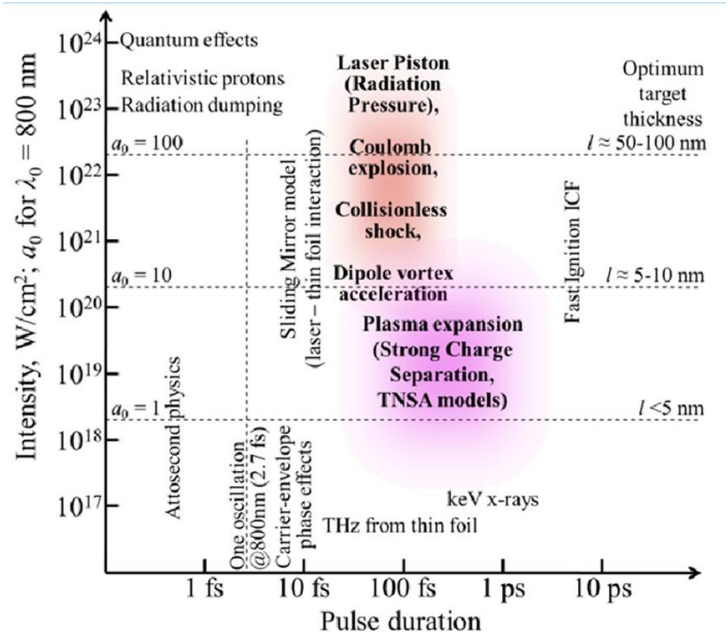

H. Daido et al Rep. Prog. Phys. 75 056401 (2012)

Most commn properties in Laser-accelerated protons:

→ Broad energy spectra (exponential-like)
→ Ultrashort duration near the source
→ Up to 10^{13} accelerated protons
→ Energy dependent beam divergence

Typical TNSA spectrum

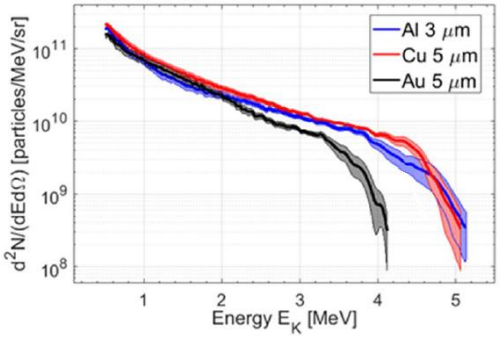

Laser Driven Ion Acceleration

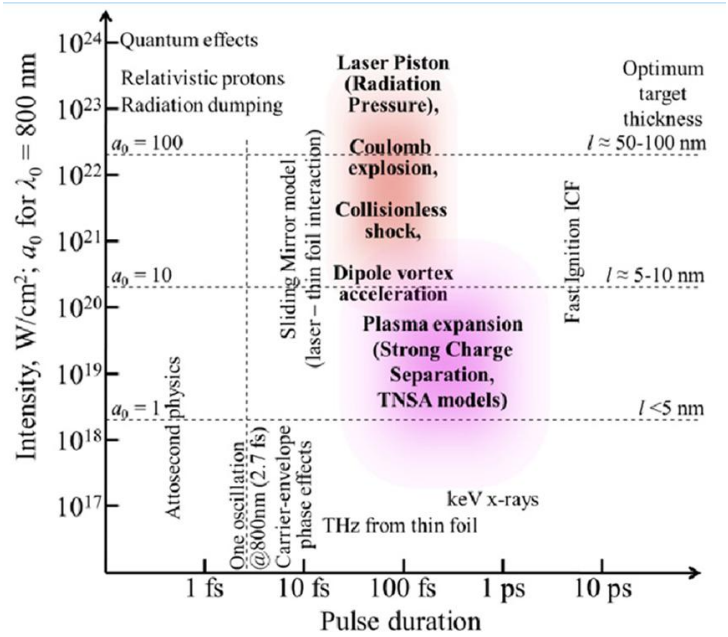

H. Daido et al Rep. Prog. Phys. 75 056401 (2012)

Most commn properties in Laser-accelerated protons:

→ Broad energy spectra (exponential-like)
→ Ultrashort duration near the source
→ Up to 10^{13} accelerated protons
→ Energy dependent beam divergence

Typical TNSA spectrum

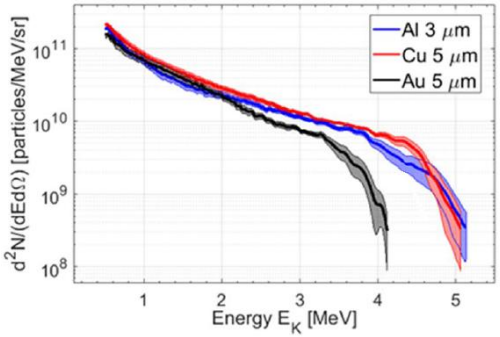

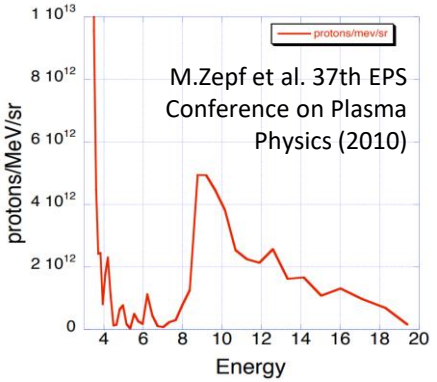

But there are exception, RPA and CSA provide peaked spectra

Application of Laser-driven protons

Material Science

→ Damage study
→ Ion Beam Analysis:
Particle Induced X-Ray Emission

Medical

→ Hadrontherapy
→ Radioisotope production for PET scan

Neutron science

→ Compact neutron source

Fusion

→ Fast Ignition Scheme
→ Proton-Boron scheme

And many others….

Application of Laser-driven protons

Material Science

→ Damage study

→ **Ion Beam Analysis:**
Particle Induced X-Ray Emission

Laser-driven proton beam is used to irradiate the sample to characterize. The energetic particles generates inner-shell vacancies with subsequent emission of characteristic radiation during the de-excitation.

Medical

→ Hadrontherapy

→ **Radioisotope production for PET scan**

Laser-driven proton beam is used to irradiate a volume of enriched water inducing the $^{18}O(p,n)^{18}F$ reaction.

Neutron science

→ Compact neutron source

Fusion

→ Fast Ignition Scheme

→ Proton-Boron scheme

And many others….

Particle Induced X-ray Emission

Energetic particles are used to irradiate the sample to characterize. The impinging particles interacting with the material generate inner-shell vacancies as a consequence of the ejection of an electron. The vacancy is filled via the transition from an upper level with **subsequent emission of characteristic radiation** during the de-excitation.

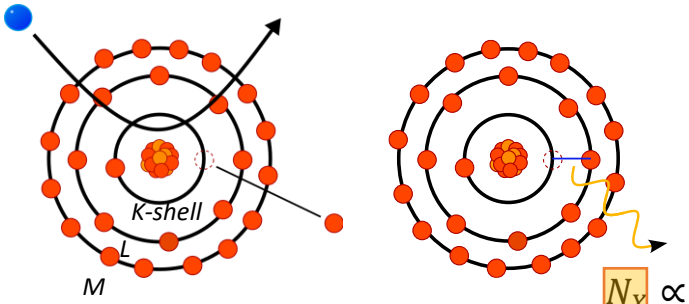

$$N_X \propto N_{el} \int dE N_p(E) \sigma_K(E)$$

The Analysis of the emitted characteristic radiation allows to retrieve both the chemical elements in the sample and their concentrations.

Proton energies in the range 2-5 MeV are suitable for this application

Technique relevant for Cultural Heritage, Industry, biology, forensic analysis…

Several shots are needed to reach resolution comparable to existing technique → toward high rep rate

Particle Induced X-ray Emission

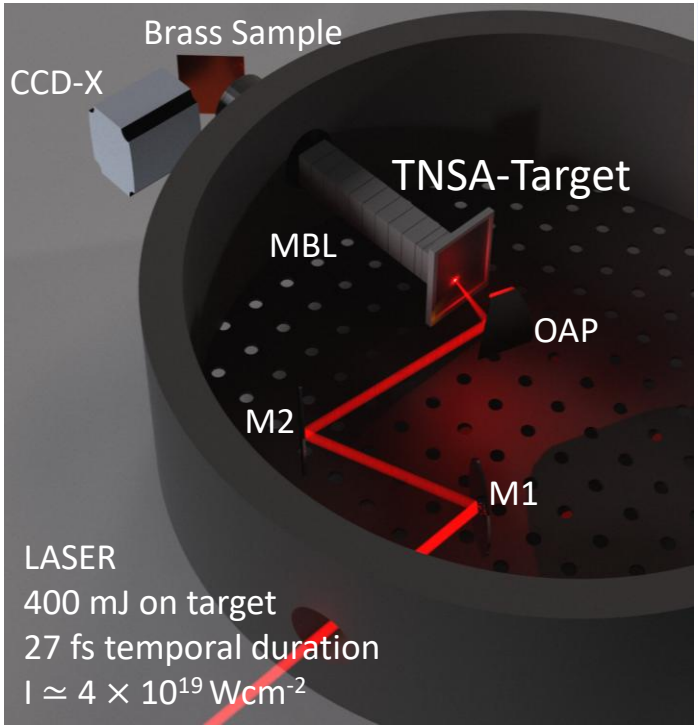

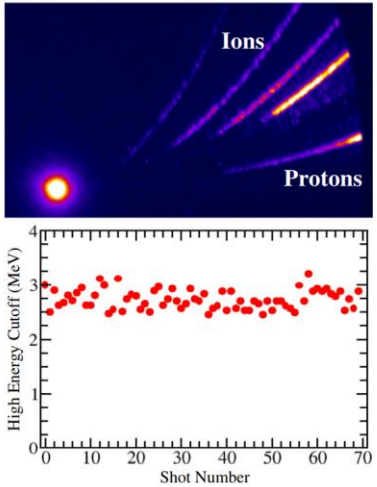

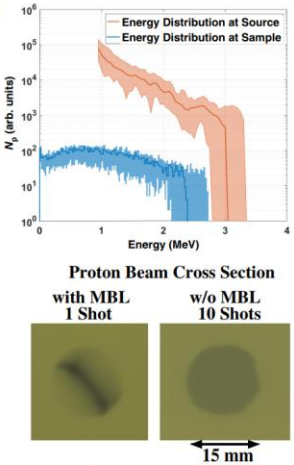

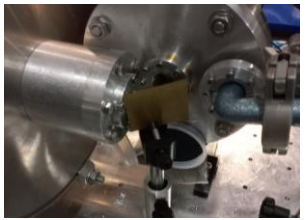

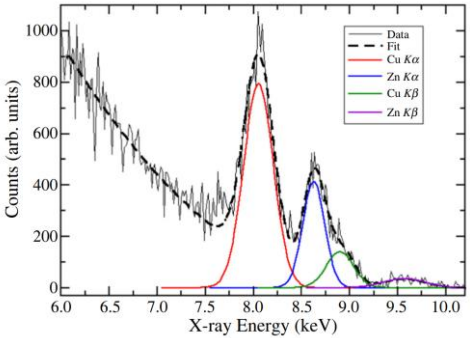

$$\frac{N_{PIXE,Cu}}{N_{PIXE,Zn}} = \frac{Y_{Cu}}{Y_{Zn}} \frac{\overline{\sigma_{Zn}}}{\overline{\sigma_{Cu}}}$$

$$\bar{\sigma} = \frac{\int N_p(E)\sigma(E)dE}{\int N_p(E)dE}$$

TABLE I. Elemental composition of the brass sample from EBL-PIXE and EDS measurements.

Technique	Copper (%)	Zinc (%)
EBL PIXE	67.8(2.5)	32.2(2.5)
EDS	69.1(1.0)	30.9(1.0)

M. Salvadori et al, Phys. Rev. Applied 21, 064020 (2024), F. Brandi et al., Appl. Sci., 11(14), 6358 (2021)

Radioisotope production for PET

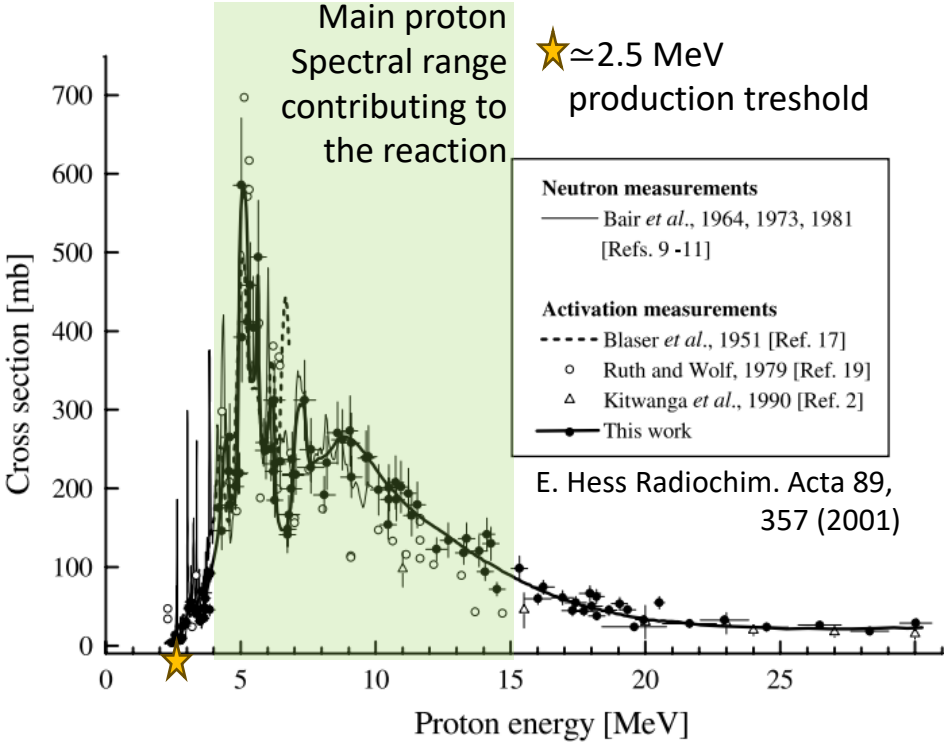

E. Hess Radiochim. Acta 89, 357 (2001)

Short-lived radioisotope production for Positron Emission Tomography (PET) ^{11}C , ^{18}F , ^{13}N , ^{15}O …

Sample of enriched water

$$^{18}_{8}O + {}^{1}_{1}p \rightarrow {}^{18}_{9}F + {}^{1}_{0}n + \gamma$$

Laser-driven proton source

on site and **on demand** production

Fluorine-18 combined with 2-deoxyglucose: **FDG** → FDG absorbed and 18F decays:

$$^{18}_{9}F \rightarrow {}^{0}_{1}e + {}^{18}_{8}O$$

$^{0}_{1}e$ annihilates emitting 2γ with 511 keV energy in opposite directions

No γ emission during the decay
$\tau_{\frac{1}{2}} \simeq 110$ min: reduced patient exposition
Non toxic
$^{0}_{1}e$ low energy, short range before annihilation

M. Conti et al. EJNMMI Physics 3, 8 (2016), M. Seimetz et al. IEEE –NSS/MIC (2015), Z. Sun AIP Advances 11, 040701(2021)

Radioisotope production for PET

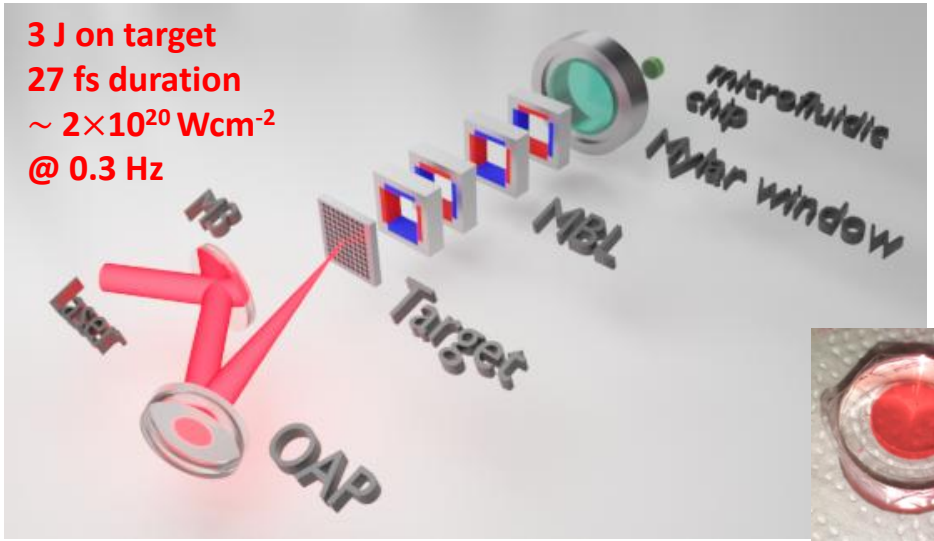

Production of small (single-patient), «on demand» doses using microfluidic chips

sample	Irradiation	Activity
15.6 uL of [^{18}O]-H_2O @98% 50 um Mylar window	85 shots accum. 45 minutes 0.03 Hz	5 (0.6) Bq

Radioisotope production for PET

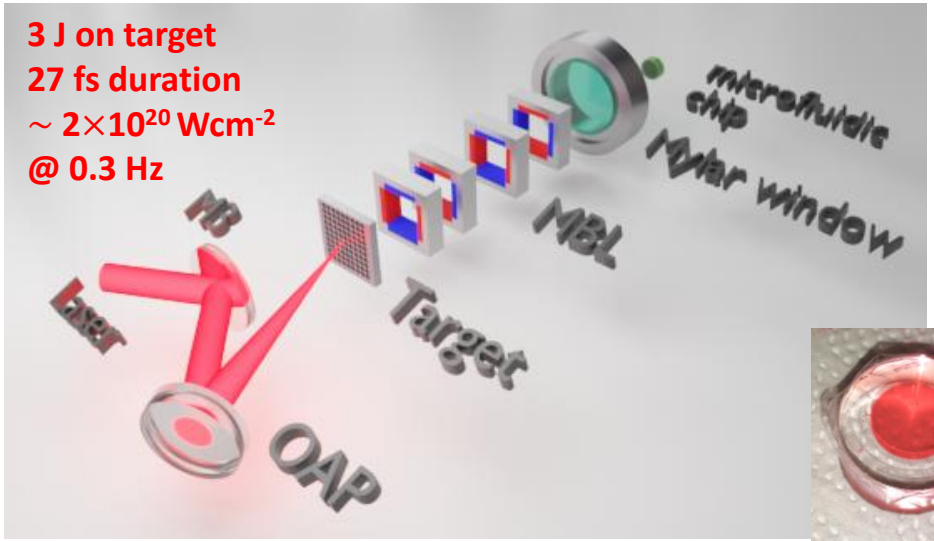

Production of small (single-patient), «on demand» doses using microfluidic chips

Results used as benchmark for Montecarlo Simulation to evaluate the capabilities in terms of sample activation employing the 1J, 25 fs laser operating at 100 Hz (currently under procurement)

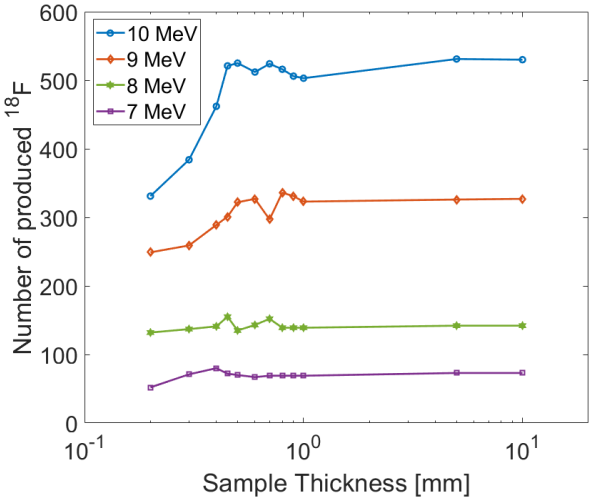

Tens of MBq activities are foreseen

Suitable to be used with novel Total Body PET machine

sample

15.6 uL of [^{18}O]-H_2O @98%

50 um Mylar window

Irradiation

85 shots accum.

45 minutes

0.03 Hz

Activity

5 (0.6) Bq

CONCLUSION

A (very) brief description of the main mechanisms underlying particle acceleration driven by laser has been given. For electrons we focus on Laser-wakefield acceleration in the bubble regime exploiting self and ionization injection. For protons, Target Normal Sheath Acceleration has been taken as reference, being the most studied and robust technique, since routinely achievable in laboratories.

Laser-driven particle accelerators can be fruitfully used for diverse applications ranging from material studies for cultural heritage to medicine. In this talk a brief overview of those that are being explored at the Intense Laser Irradiation Laboratory of the CNR-INO in Pisa was given.

Ongoing laser systems and laboratory major upgrade aims primarily at enabling applications requiring a high average flux of particles exploiting high repetition rate systems.

Infrastructure Development

This work was supported by the PNRR MUR project IR0000016-I-PHOQS, funded by the European Union –Next Generation EU.

I-PHOQS
INTEGRATED INFRASTRUCTURE INITIATIVE IN PHOTONIC AND QUANTUM SCIENCES

And EuPRAXIA Advanced Photon Sources - EuAps (IR0000030, CUP I93C21000160006).

EuPRAXIA
Advanced Photon Sources

Laser Development

This work was supported by the EU Horizon IFAST, under Grant Agreement No.101004730

iFAST

Experimental investigation on biomedicine

This work was supported by the PNRR MUR project IR0000016-I-PHOQS, funded by the European Union –Next Generation EU.

THE Tuscany Health Ecosystem

Laser-Driven electron Acceleration: wakefield generation

According to the laser intensity it is possible to distinguish among two different regimes:

- Linear regime $a_o = \frac{eE_L}{m_e \omega_L c} \ll 1$

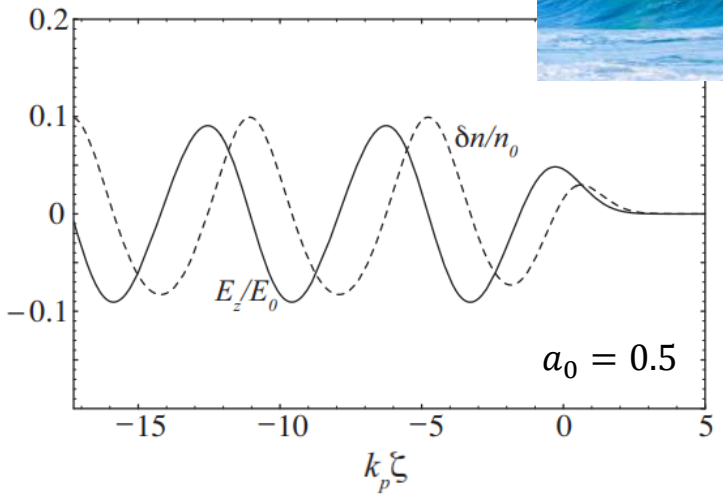

The density perturbation, as well as the axial wakefield E_z (accelerating field), have a sinusoidal form characterized by the plasma wavelength

$$\lambda_p[\mu m] \simeq 33 \times (n_e[10^{18} cm^{-3}])^{-\frac{1}{2}}$$

The amplitude of the accelerating field:

$$E[Vm^{-1}] \simeq 96(n_e[cm^{-3}])^{\frac{1}{2}} \frac{\delta n_e}{n_e}$$

$$\rightarrow E_0[Vm^{-1}] \simeq 96(n_e[cm^{-3}])^{\frac{1}{2}}$$

Cold non-relativistic wakebreaking field

E. Esarey et al., RevModPhys 81 (2009)

Laser-Driven electron Acceleration: wakefield generation

According to the laser intensity it is possible to distinguish among two different regimes:

- Linear regime $a_o = \frac{eE_L}{m_e \omega_L c} \ll 1$

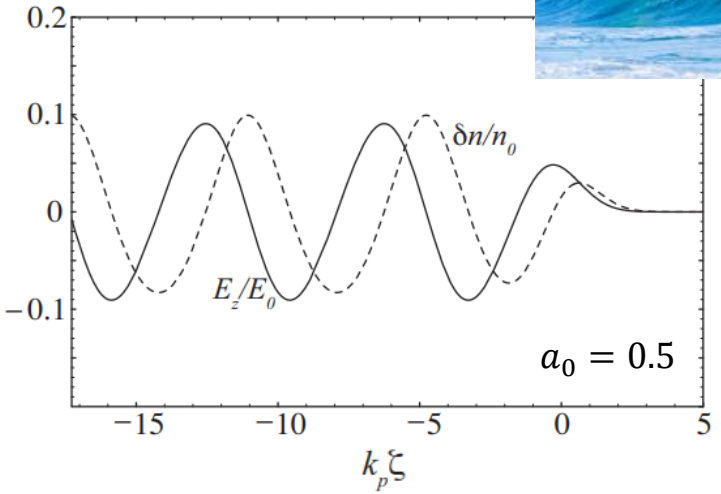

- Non- Linear regime $a_o \geq 1$

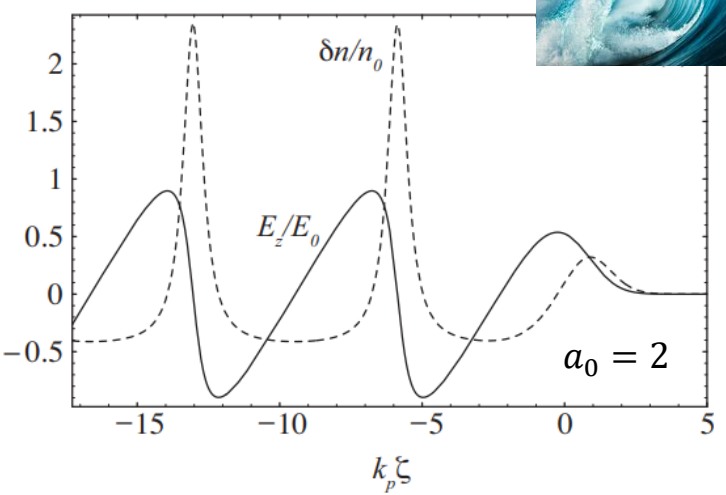

E. Esarey et al., RevModPhys 81 (2009)

Laser-Driven electron Acceleration: wakefield generation

According to the laser intensity it is possible to distinguish among two different regimes:

- Non- Linear regime $a_o \geq 1$

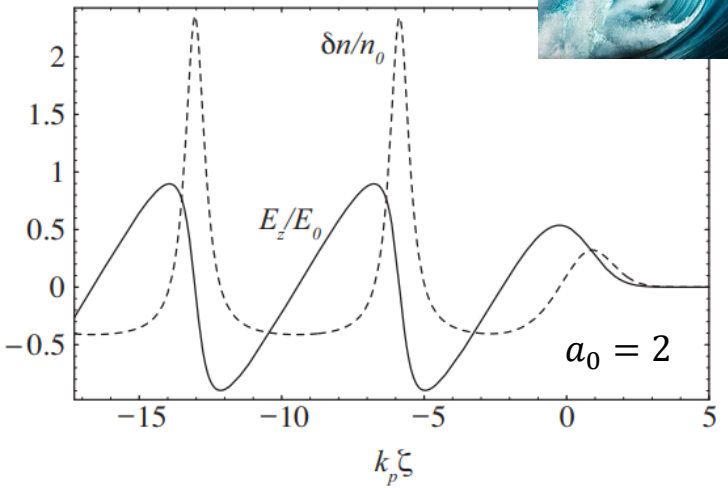

E. Esarey et al., RevModPhys 81 (2009)

LWFA: main limitations and maximum energy gain

Diffraction $w(z) = w_o\sqrt{1+\left(\frac{Z_R}{z}\right)^2}$ $Z_R = \frac{\pi\omega_0}{\lambda}$

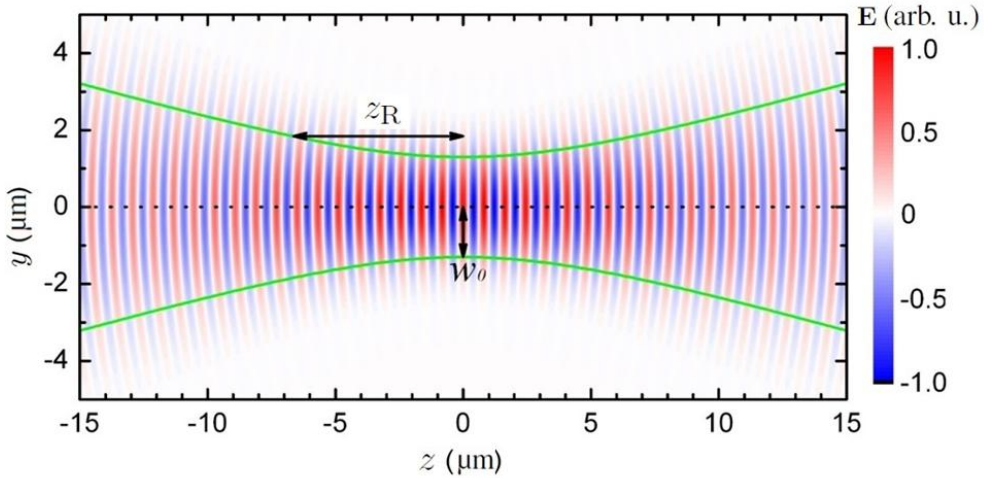

LWFA: main limitations and maximum energy gain

Diffraction $w(z) = w_o\sqrt{1+\left(\frac{Z_R}{z}\right)^2}$ $Z_R = \frac{\pi\omega_0}{\lambda}$

Dephasing Lenght L_d

As the electron gain energy it will approach the limit $v_z \to c$. Since the phase velocity of the plasma wave is lower than the speed of light, the electrons will reach a decelerating region of the plasma wave

$L_d \simeq \frac{\lambda_p^3}{2\lambda_L^2}$ per $a_0 \ll 1$ $L_d \simeq \frac{\lambda_p^3}{2\lambda_L^2}\frac{\sqrt{2}}{\pi}\frac{a}{N_P}$ per $a_0 \gg 1$

Pump Depletion L_{dp}

As the laser propagates in the plasma, it transfers its energy to the plasma wave. The pump depletion length is defined as the distance over which the laser has lost its power

$L_{dp} \simeq \frac{\lambda_p^3}{\lambda_L}\frac{2}{a_0}$ per $a_0 \ll 1$ $L_{dp} \simeq \frac{\lambda_p^3}{\lambda_L^2}\frac{\sqrt{2}}{\pi}a_0$ per $a_0 \gg 1$

Maximum energy gain: an ideal estimate

→ Can be obtained multiplying the accelerating field with the maximum accelerating length, i.e. the shorter between L_d, L_{dp} and $Z_R \to \Delta W = eE_Z L_{acc}$

Diffraction limited $\Delta W_R(MeV) \simeq 740\frac{\lambda}{\lambda_p}\left(1+\frac{a_0^2}{2}\right)^{-\frac{1}{2}}P(TW)$

Issue mitigation → **Relativistic Self Focusing**

Preformed plasma channel

Beam Loading

The accelerated electron bunch will, in turn, generate a wake. This will be out of phase with respect to the laser-driven wake → limitation on beam current and bunch quality

VHEE spectrum UHDR

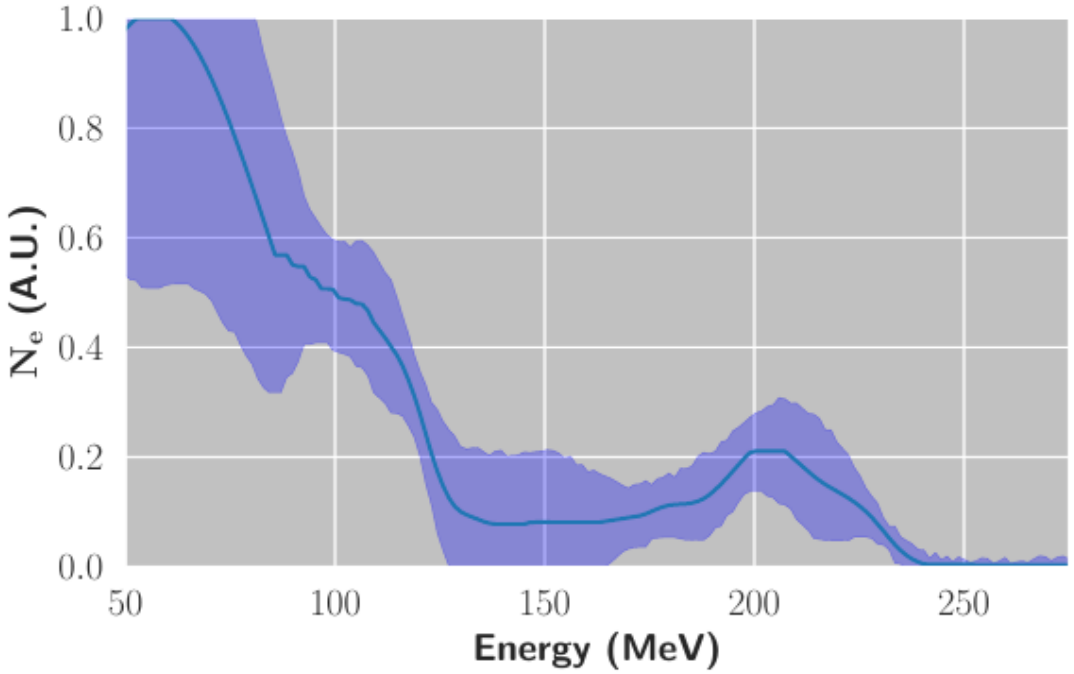

Electron Beam manipulation: Magnetic Beamline

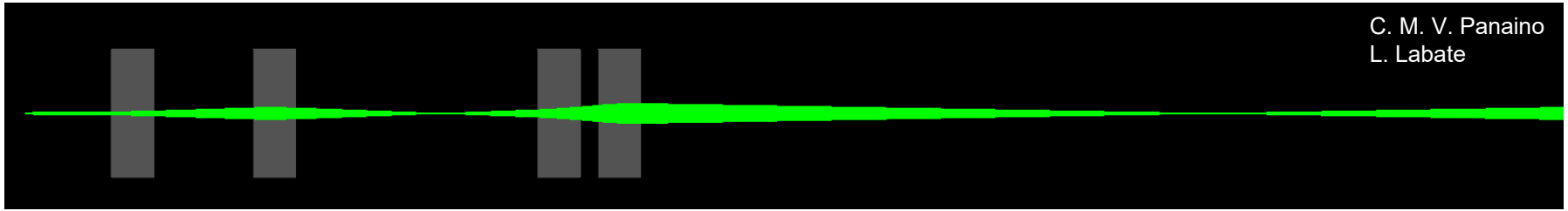

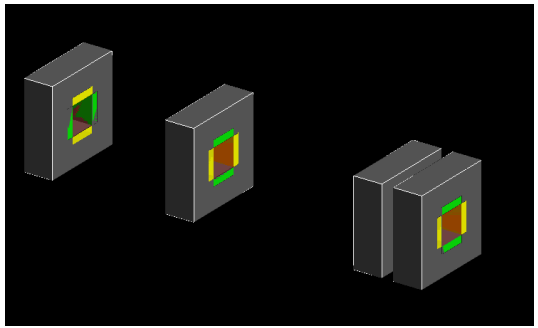

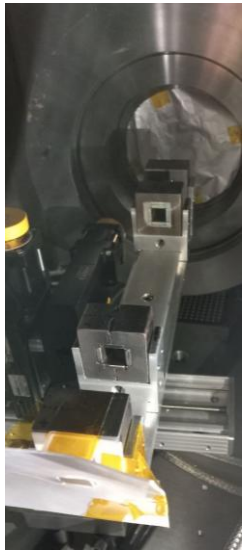

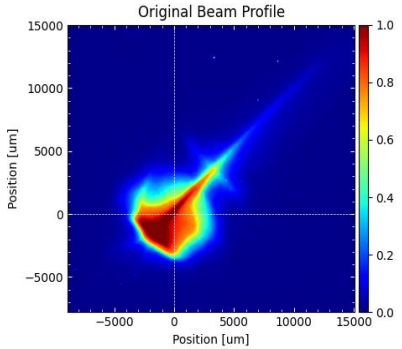

Magnetic Beamline main effects:

- Enhance pointing stability
- Energy selector
- Reducing beam size

Pointing stability deviations:

$\sigma_x = 0.55$ mm, $\sigma_y = 0.46$ mm

Average beam size:

0.60×0.44 cm